

Gamow-Teller strength distributions in Fe and Ni stable isotopes

P. Sarriuguren, E. Moya de Guerra, and R. Álvarez-Rodríguez

*Instituto de Estructura de la Materia,
Consejo Superior de Investigaciones Científicas,
Serrano 123, E-28006 Madrid, Spain*

We study Gamow-Teller strength distributions in some selected nuclei of particular Astrophysical interest within the iron mass region. The theoretical framework is based on a proton-neutron Quasiparticle Random Phase Approximation built on a deformed selfconsistent mean field basis obtained from two-body density-dependent Skyrme forces. We compare our results to available experimental information obtained from (n, p) and (p, n) charge exchange reactions.

I. INTRODUCTION

It is well known [1,2] that nuclear β -decay and electron capture processes are very important mechanisms to understand the late stages of stellar evolution. These processes are essential ingredients in calculations of supernova formation. In particular, Gamow-Teller (GT) properties of nuclei in the region of medium masses around $A=56$ are of special importance because they are the main constituents of the stellar core in presupernovae formations.

It is clear that due to the extreme conditions of densities and temperatures that hold in the stellar scenarios, involving highly unstable nuclei as well, most of those properties cannot be measured directly. Therefore, the GT strength distributions must be estimated in many cases by model calculations. Collapse simulations of supernovae have been carried out so far by treating the GT transition rates in a rather qualitative way. For example, it is a common practice [2] to assume that the whole GT strength resides in a single resonance whose energy relative to the daughter ground state is parametrized phenomenologically, taking the total GT strength from the single-particle model.

In the last decades, GT_+ strength distributions on nuclei in the mass region $A=50-65$ have been studied experimentally via (n, p) charge exchange reactions at forward angles [3–7]. The (n, p) charge-exchange reaction is one of the best efficient ways to extract the GT_+ strength in nuclei. For incident energies above 100 MeV, the isovector spin-flip component of the effective interaction is dominant and the cross sections arise mainly from spin-isospin transitions. At forward angles and low excitation energies in the final nucleus, the momentum transfer is small and therefore the reaction cross section is dominated by the GT operator with $\Delta T = 1, \Delta L = 0, \Delta J^\pi = 1^+$. The cross section, extrapolated to zero momentum transfer, is proportional to the β -decay strength between the same states. Charge exchange reactions at small momentum transfer can therefore be used to study GT strength distributions when β -decay is not energetically possible.

The experimental data [3–7] show that the total GT_+ strength is strongly quenched and fragmented over many final states, as compared to the independent particle model. This is caused by residual nucleon nucleon correlations. The data also indicate a systematic misplacement of the GT centroid adopted in the parameterizations of Ref. [2]. An improved theoretical description of the stellar weak interaction rates, treating the nuclear structure problem more accurately, is then required. Shell Model Montecarlo [8] and large scale Shell Model diagonalization calculations [9,10] have been already used to derive the stellar rates. The reliability of the latter diagonalization methods was demonstrated [10] by comparing the calculated GT_+ strength distributions of nuclei in the iron mass region with the corresponding experimental distributions in the whole range of excitation energies, as obtained from (n, p) charge exchange reactions.

This comparison with experiment is important not only for the direct determination of the GT_+ strength distributions in stable nuclei, but also for the calibration of model calculations that are used in a further step to estimate the strength distributions for unstable nuclei or the strength distributions of nuclei under high temperature and density conditions, where no experimental information is available. In this line of thought, it is also important to compare to the data set [3–7] the predictions of other microscopic models that, though may not be as accurate as the Shell Model calculations of Caurier et al. [10] in this mass region ($A \sim 60$), have at present a wider range of applicability. This is particularly the case of the proton-neutron quasiparticle random phase approximation (pnQRPA) with separable Gamow-Teller (V_{GT}) residual interaction. The purpose of this work is to test to what extent this approach, not limited by mass number, can account for the above mentioned set of data.

The pnQRPA method with a separable GT (or Fermi, V_F) interaction was first proposed and applied in Ref. [11], on a spherical harmonic oscillator basis, and then it was extended to deformed nuclei [12] using deformed phenomenological single-particle basis. Like standard RPA, for a repulsive residual interaction, the method is correct both in the weak coupling and strong coupling limits. The strong coupling limit of pnQRPA gives the correct result by yielding the multiplet (supermultiplet) structure associated with the V_F (V_{GT}) force, respectively [11]. Other attractive features of the pnQRPA method are that the linear energy weighted sum rule is conserved and that Ikeda sum rule is fulfilled. Further refinements to the pnQRPA formalism have been introduced along the years (see in particular [13,14] and references therein), including, in particular, particle-particle residual interactions [15–17].

Weak interaction rates and nuclear properties relevant for astrophysical applications within the pnQRPA have also been reported [18], but a detailed comparison of the predictions of this model with experimental distributions in the iron mass region is still missing. In Refs. [14,19–21] we performed pnQRPA calculations based on a deformed Hartree-Fock basis obtained from density dependent Skyrme forces and pairing correlations. In this work we extend those calculations to the iron mass region.

The paper is organized as follows: In the next Section we describe briefly the theoretical formalism used to calculate the GT strength distributions. In Section 3 we present and discuss the results obtained and compare them with experiment. In Section 4 we summarize the main conclusions.

II. THEORETICAL FORMALISM

In a previous work [14,19–21] we studied ground state and β -decay properties of even-even and odd-A exotic nuclei on the basis of a deformed selfconsistent HF+BCS+pnQRPA calculation with density dependent effective interactions of Skyrme type, including $T_z = \pm 1$ pairing correlations in BCS approximation. Our purpose here is to extend these calculations to stable nuclei in the iron mass region and to investigate up to what extent this approach is able to reproduce the experimental information extracted from the charge exchange reactions in the Fe-Ni region.

The theory involved in the microscopic calculations can be seen in detail in Refs. [14,19–21]. For the solution of the Hartree-Fock (HF) equations we follow the McMaster procedure [22] that is based in the formalism developed in Ref. [23]. Time reversal and axial symmetry are assumed. The single-particle wave functions are expanded in terms of the eigenstates of an axially symmetric harmonic oscillator in cylindrical coordinates using eleven major shells in the expansion. The method also includes pairing between like nucleons in the BCS approximation with fixed gap parameters for protons Δ_π , and neutrons Δ_ν , which are determined phenomenologically from the odd-even mass differences through a symmetric five term formula involving the experimental binding energies [24].

For odd-A nuclei, the fields corresponding to the different interactions were obtained from the corresponding self-consistent field of the closest even-even nucleus, selecting the orbital occupied by the odd nucleon among those around Fermi level, according to the experimental spin and parity.

We study first the energy surfaces as a function of deformation for all the isotopes under study here. For that purpose, we perform constrained HF calculations with a quadrupole constraint [25] and minimize the HF energy under the constraint of keeping fixed the nuclear deformation. The GT distributions in the next section are then calculated for the equilibrium shape of each nucleus obtained in this way, that is, for the solution, in general deformed, for which we obtain the minimum in the energy surface.

We can see in Fig. 1 the total HF+BCS energy as a function of deformation for the nuclei under study in this work with three different Skyrme interactions: SG2 [26], Sk3 [27], and the more recent SLy4 [28]. For an easier comparison, the origin is different in the vertical axis for the three forces but the distance between ticks corresponds always to 1 MeV. As we can see from the figure, the three forces predict a similar behavior in most cases. Thus, SG2 and SLy4 produce a shallow minimum around the spherical shape in ^{54}Fe with a slightly prolate shape favored energetically. On the other hand, Sk3 force gives a spherical equilibrium shape. In the case of ^{56}Fe , the three forces favor a prolate solution with another oblate minimum at about 1 MeV higher. ^{58}Ni is spherical according to the results obtained from the three forces considered. In the case of Ni isotopes, we observe that the SLy4 interaction predicts spherical shapes in ^{58}Ni , ^{60}Ni and ^{62}Ni , although the minimum is shallower in the latter cases. In ^{64}Ni a slightly oblate shape is predicted with this force. The SG2 and Sk3 interactions produce again a spherical shape in ^{58}Ni , but contrary to the force SLy4, a shape coexistence between oblate and prolate shapes is predicted in $^{60,62,64}\text{Ni}$.

We can also see in Table 1 a comparison of experimental and calculated charge radii (r_c) and quadrupole moments (Q_0). Experimental values are from Refs. [29] in the case of r_c and from [30] in the case of Q_0 . The calculated values are obtained from deformed HF+BCS calculations with the force SG2.

To describe GT transitions we add to the mean field a spin-isospin residual interaction. This interaction contains two parts, particle-hole (ph) and particle-particle (pp). The ph part is mainly responsible for the position and structure of the GT resonance [16,19] and, in principle, it could be derived selfconsistently from the same energy density functional

as the HF equation. After averaging the force over the nuclear volume, it can be written in a separable form [14,19], with a coupling strength χ_{GT}^{ph} determined by the Skyrme parameters. By taking separable GT forces, the energy eigenvalue problem reduces to find the roots of an algebraic equation.

Since the GT giant resonance for stable nuclei can be measured from charge exchange reactions, it is a common practice to fit the coupling strength χ_{GT}^{ph} to reproduce the energy of the resonance. Several parameterizations have been proposed to reproduce these energies in large scale calculations. Nevertheless, one should take into account that the coupling strengths obtained in this way depend on the model used for single particle and correlated wave functions and on the set of experimental data considered. Thus, values of the coupling strengths obtained from a given fitting procedure cannot be safely extrapolated to other cases.

The particle-particle part is a neutron-proton pairing force in the $J^\pi = 1^+$ coupling channel. We introduce this interaction in the usual way [15,16,20], that is, in terms of a separable force with a coupling constant κ_{GT}^{pp} , which is usually fitted to reproduce the half-lives.

Both *ph* and *pp* residual interactions reduce the GT strength. Calculations within a single major shell in both QRPA and configuration mixing Shell Model were made in Ref. [31], where it was shown that the quenching produced by QRPA calculations is similar to that found in Shell Model including all possible $0p0h$ and $2p2h$ configurations. The residual forces produce also a displacement of the GT strength, which is to higher energies in the case of the repulsive *ph* force and to lower energies in the case of the attractive *pp* force.

The optimum set of coupling strengths $(\chi_{GT}^{ph}, \kappa_{GT}^{pp})$ could be chosen following a case by case fitting procedure and we will get different answers depending on the nucleus, shape and Skyrme force. However, since the purpose here is to test the ability of pnQRPA models to account for the GT strength distributions in the iron mass region with as few free parameters as possible, we have chosen to use the same coupling strengths for all the nuclei considered in this work.

The pnQRPA phonon operator for GT excitations in even-even nuclei is written as

$$\Gamma_{\omega_K}^+ = \sum_{\pi\nu} [X_{\pi\nu}^{\omega_K} \alpha_\nu^+ \alpha_\pi^+ - Y_{\pi\nu}^{\omega_K} \alpha_\nu^- \alpha_\pi^-], \quad (2.1)$$

where π and ν stand for proton and neutron, respectively, α^+ (α) are quasiparticle creation (annihilation) operators, ω_K are the RPA excitation energies, and $X_{\pi\nu}^{\omega_K}, Y_{\pi\nu}^{\omega_K}$ the forward and backward amplitudes, respectively. It satisfies

$$\Gamma_{\omega_K} |0\rangle = 0; \quad \Gamma_{\omega_K}^+ |0\rangle = |\omega_K\rangle. \quad (2.2)$$

Solving the pnQRPA equations [12,14,16], the GT transition amplitudes in the intrinsic frame of even-even nuclei connecting the QRPA ground state of the parent nucleus $|0\rangle$ to one phonon states in the daughter nucleus $|\omega_K\rangle$, are given by

$$\langle \omega_K | \beta_K^\pm | 0 \rangle = \mp M_\pm^{\omega_K}, \quad (2.3)$$

where $\beta_K^\pm = \sigma_K \tau^\pm$, $K = 0, \pm 1$, and

$$M_-^{\omega_K} = \sum_{\pi\nu} (q_{\pi\nu} X_{\pi\nu}^{\omega_K} + \tilde{q}_{\pi\nu} Y_{\pi\nu}^{\omega_K}); \quad M_+^{\omega_K} = \sum_{\pi\nu} (\tilde{q}_{\pi\nu} X_{\pi\nu}^{\omega_K} + q_{\pi\nu} Y_{\pi\nu}^{\omega_K}), \quad (2.4)$$

with

$$\tilde{q}_{\pi\nu} = u_\nu v_\pi \Sigma_K^{\nu\pi}; \quad q_{\pi\nu} = v_\nu u_\pi \Sigma_K^{\nu\pi}; \quad \Sigma_K^{\nu\pi} = \langle \nu | \sigma_K | \pi \rangle, \quad (2.5)$$

where v 's are occupation amplitudes ($u^2 = 1 - v^2$). The single particle wave functions, energies, and occupation probabilities are generated from the selfconsistent deformed mean field obtained with the Skyrme force. To calculate GT strengths we have considered the force SG2 that has been successfully tested against spin-isospin excitations in spherical [26] and deformed nuclei [14,19–21,32]. Comparison to calculations obtained with other Skyrme forces have been made in Refs. [14,19], showing that the results do not differ in a significant way.

When the parent nucleus has an odd nucleon, the ground state can be expressed as a one quasi-particle state in which the odd nucleon occupies the single-particle orbit of lowest energy. Then two types of transitions are possible. One type is due to phonon excitations in which the odd nucleon acts only as a spectator. In the intrinsic frame, the transition amplitudes are in this case basically the same as in the even-even case but with the blocked spectator excluded from the calculation. The other type of transitions are those involving the odd nucleon state, which are treated [12,16,21] by taking into account phonon correlations in the quasiparticle transitions in first order perturbation.

Once the intrinsic amplitudes $\langle f | \beta_K^\pm | i \rangle$ are calculated, the Gamow-Teller strength B_{GT} for a transition $I_i \rightarrow I_f$ can be obtained as

$$\begin{aligned}
B_{GT}^{\pm} &= \sum_{M_i, M_f, \mu} |\langle I_f M_f | \beta_{\mu}^{\pm} | I_i M_i \rangle|^2 \\
&= \delta_{K_i, K_f} [\langle I_i K_i 10 | I_f K_f \rangle \langle \phi_{K_f} | \beta_{+1}^{\pm} | \phi_{K_i} \rangle \\
&\quad + \delta_{K_i, 1/2} (-1)^{I_i - K_i} \langle I_i - K_i 11 | I_f K_f \rangle \langle \phi_{K_f} | \beta_{+1}^{\pm} | \phi_{K_i} \rangle]^2 \\
&\quad + \delta_{K_f, K_i + 1} \langle I_i K_i 11 | I_f K_f \rangle^2 \langle \phi_{K_f} | \beta_{+1}^{\pm} | \phi_{K_i} \rangle^2 \\
&\quad + \delta_{K_f, K_i - 1} \langle I_i K_i 1 - 1 | I_f K_f \rangle^2 \langle \phi_{K_f} | \beta_{-1}^{\pm} | \phi_{K_i} \rangle^2,
\end{aligned} \tag{2.6}$$

in units of $g_A^2/4\pi$. To obtain this expression we have used the initial and final states in the laboratory frame expressed in terms of the intrinsic states $|\phi_K\rangle$ using the Bohr-Mottelson factorization [33].

Eq. (2.6) can be particularized for even-even parent nuclei. In this case $I_i = K_i = 0$, $I_f = 1$, and $K_f = 0, 1$.

$$B_{GT}^{\pm} = \frac{g_A^2}{4\pi} \left\{ \delta_{K_f, 0} \langle \phi_{K_f} | \beta_0^{\pm} | \phi_0 \rangle^2 + 2\delta_{K_f, 1} \langle \phi_{K_f} | \beta_1^{\pm} | \phi_0 \rangle^2 \right\}. \tag{2.7}$$

III. RESULTS

In this Section we present and discuss the results obtained for the GT strength distributions and summed strengths. The results correspond to pnQRPA calculations with the Skyrme force SG2 and they have been performed for the nuclear shape that minimizes the HF energy. Before discussing the figures we note that the GT strength distributions are plotted versus the excitation energy of the daughter nucleus. The distributions of the GT strength have been folded with $\Gamma = 2$ MeV width Gaussians to account for the finite experimental resolution as it was done in Refs. [8–10], so that the original discrete spectrum is transformed into a continuous profile. The theoretical GT distributions in those figures have been quenched with a factor $[(g_A/g_V)_{\text{eff}}/(g_A/g_V)_{\text{free}}]^2 = (0.7)^2$, which is standard for transitions involving the spin operator [34]. The observed GT strength in charge exchange reactions is less than the expected strength from the Ikeda sum rule.

This quenching factor is similar to that found in spin $M1$ transitions in stable nuclei, where $g_{s,\text{eff}}$ is also known to be approximately $0.7 g_{s,\text{free}}$.

As we have already mentioned, the two coupling strengths of the ph and pp residual interactions have been determined to reproduce the positions of the experimental GT_+ resonances as obtained from the (n, p) reactions. This has been done in a global way, choosing $\chi_{GT}^{ph} = 0.10$ MeV and $\kappa_{GT}^{pp} = 0.05$ MeV, as the best set of values within a deformed HF basis with the force SG2 for the observed resonances in the set of nuclei considered in this work. We note that the value of χ_{GT}^{ph} , which mainly determines the position of the resonance, is smaller than the typical values expected from systematic fits [17] or from consistency with the SG2 mean field [14,19–21]. This feature was already pointed out in Ref. [35], where the coupling strengths χ_{GT}^{ph} needed to reproduce the GT giant resonances were found to be smaller than the fitted A^{-1} law, in the mass region under consideration in this work.

The results obtained for the GT_+ strength distributions can be seen in Fig.2. Plotted downward are the results of uncorrelated two-quasiparticle (HF+BCS) calculations, both individual and folded strengths. Plotted upward are the experimental data, accumulated in 1 MeV bins (dots with error bars), as well as the GT_+ strengths obtained from correlated two-quasiparticle (HF+BCS+ pnQRPA) calculations. The agreement with experiment is in general quite satisfactory. We can see that the experimental GT_+ strength distributions are fragmented over many states and that the centroids and widths of the distributions are well reproduced in our calculations. However, experimental GT_+ distributions show a tendency to build up a second peak beyond ~ 6 MeV, which is not seen in the theoretical calculations. This indicates that in order to reproduce these strengths at high energy, one should include higher correlations in the theoretical calculations. The total GT_+ strength contained below the measured excitation energies can be seen in Table 2. We can see that the summed strengths in HF+BCS+pnQRPA agree better with experiment, but are still somewhat larger than the experimental ones.

We observe that the inclusion of the pnQRPA correlations reduces the total HF+BCS strength by about 20-40%, depending on the nucleus, improving always the comparison with experiment. However, even the simpler HF+BCS calculation with the force SG2 produces quite good results in most cases. This is not only true for the GT_+ strength distributions, but also for the summed strengths. Our theoretical summed strengths are in general somewhat larger than those from Shell Model calculations [8,10], however, in some instances compare better to experiment. This is the case of ^{64}Ni , where Shell Model calculations [8,10] give strengths considerably lower than experiment.

Though the GT_+ strength distributions obtained from full Shell Model calculations by Caurier et al. [10] may agree better with experiment in some details, the present HF+BCS+pnQRPA results are, on the overall, of comparable

quality. The problem of missing theoretical strength at high energy (that was found in Shell Model calculations) persist here, although we get more strength at higher energy than Shell Model [10] because of the higher N-shell mixing contained in HF+BCS+pnQRPA.

The peaks of the observed GT_+ strength distributions in the odd-A nuclei considered are found to be consistently at higher excitation energies in the daughter nucleus as compared to their even-even partners. This feature is well described in our calculations and the reason, which was discussed in Ref. [21], is related to the energy needed to break a Cooper pair.

Although the stellar electron captures and β -decays are more sensitive to the distribution of the GT_+ strength, the GT_- strength distributions play also a non negligible role in the calculation of the stellar weak interaction rates and it is also of interest the study of their distributions. In addition, this allows to study Ikeda sum rule, which is always fulfilled in our calculations, as well as the total quenching.

We plot in Fig. 3 the experimental forward-angle (p, n) cross sections from Ref. [36] because only in a few specific cases [37] the cross sections have been converted into GT_- strength distributions. We can observe the highly fragmented strength distribution obtained as well as the concentration of the strength in different energy regions depending on the nucleus. In the lower panel we can see the calculated GT_- strength distributions obtained from HF+BCS+pnQRPA calculations with the force SG2. We show three different types of results for each nucleus. The dotted lines are the HF+BCS results without including any residual interaction. The curves labeled $QRPA_1$ and $QRPA_2$ are the results obtained when we introduce the ph and pp residual interactions discussed above with two different sets of parameters for χ_{GT}^{ph} and κ_{GT}^{pp} . The dashed lines ($QRPA_1$) are obtained using the same coupling strengths we have used to calculate GT_+ strengths in Fig. 2, that is $\chi_{GT}^{ph} = 0.10$ MeV and $\kappa_{GT}^{pp} = 0.05$ MeV. For comparison we also show by solid lines ($QRPA_2$) results obtained using the coupling strengths derived from the Skyrme force following the procedure in Ref. [14] ($\chi_{GT}^{ph} = 0.43$ -0.55 MeV, depending on the nucleus), and using $\kappa_{GT}^{pp} = 0.07$ MeV. These values are close to the values derived from the parameterization of Ref. [17] ($\chi_{GT}^{ph} = 5.2/A^{0.7} = 0.28$ -0.34 MeV, $\kappa_{GT}^{pp} = 0.58/A^{0.7} = 0.032$ -0.038 MeV, depending also on the nucleus). Though here we cannot compare directly to GT_- data, and Fermi contributions are also included, the figure shows that theory reproduces the two peak structure, which is the dominant feature of data. Clearly, with the same set of parameters we also get missing GT_- strength in the high energy sector as it was the case in GT_+ .

IV. CONCLUSIONS AND FINAL REMARKS

We have applied a selfconsistent deformed HF+BCS+pnQRPA formalism with density-dependent effective Skyrme interactions to the description of the GT strength in several nuclei in the Fe-Ni mass region.

We find that the present pnQRPA calculations are able to reproduce the main features of the GT properties measured in this mass region, reinforcing confidence in the method and in its predictive power. The method had been successfully contrasted against the experimental half-lives of unstable proton rich nuclei in the $A \sim 70$ mass region on one hand, and against experimental $M1$ spin strength distributions in the rare earths region on the other. In those applications we found agreement with experiment using the Gamow-Teller strength constant (χ_{GT}^{ph}) derived consistently with the mean field from the same Skyrme interaction, following a procedure that gives an overall $1/A$ law for χ_{GT}^{ph} [14]. From phenomenological fits [35] it is known that the empirical $1/A$ law does not work well in this mass region, where fitted χ_{GT}^{ph} values are considerably lower than those suggested by the $1/A$ line. It is therefore not surprising that we find here better agreement with data with a smaller χ_{GT}^{ph} . The reasons why the overall procedure used in [14], or equivalently the $1/A$ laws do not apply here is an interesting subject for future investigation in itself. It may be connected to the fact that those methods do not take into account possible renormalization of the GT strength constant in the vicinity of shell closures. It may also be connected to particular properties of effective two-body forces of Skyrme type that have so far not been sufficiently investigated. Clearly, the fact that χ_{GT}^{ph} is small in this region implies that pnQRPA correlations are smaller than in other regions previously investigated, and that the bare two quasiparticle approximation is already a fairly good approximation here. In the latter, only deformation and $T_z = \pm 1$ pairing correlations are taken into account. We find that deformation is essential in these calculations to get the proper fragmentation of the strength, that clearly shows up and differentiates the experimental strength distributions of the different nuclei.

Although in this mass region the Shell Model calculations of Ref. [10] may be superior, and some fine details of data may be better described, we find that on the overall the agreement with experiment of present pnQRPA calculations is comparable and tend to do better in the higher energy domain ($E > 7$ MeV). However, in this domain both methods fail to reproduce data. Provided these data are unquestionable, they point out to a lack of higher order correlations (as it is particularly for pnQRPA) or to limitations of the single particle basis (as it is particularly for Shell Model) in the theoretical calculations. With these limitations in mind, the present comparison of pnQRPA to data provides a fairly sound basis to safely apply this method to the estimates of GT strengths and particularly of β -decay properties of highly unstable nuclei in other mass regions. In addition, our approach can be extended to much heavier nuclei beyond the present capability of the full Shell Model, without increasing the complexity of the calculations.

ACKNOWLEDGMENTS

This work was supported by Ministerio de Ciencia y Tecnología (Spain) under contract number BFM2002-03562. One of us (R.A.-R.) thanks Ministerio de Educación, Cultura y Deporte (Spain) for financial support.

[1] H.A. Bethe, G.E. Brown, J. Applegate, and J.M. Lattimer, Nucl. Phys. A 324 (1979) 487.

[2] G.M. Fuller, W.A. Fowler, and M.J. Newman, ApJS 42 (1980) 447; 48 (1982) 279; ApJ 252 (1982) 715; 293 (1985) 1.

[3] M.C. Vetterli, O. Häusser, R. Abegg, W.P. Alford, A. Celler, D. Frekers, R. Helmer, R. Henderson, K.H. Hicks, K.P. Jackson, R.G. Jeppesen, C.A. Miller, K. Raywood, and S. Yen, Phys. Rev. C 40 (1989) 559.

[4] T. Rönnqvist, H. Condé, N. Olsson, E. Ramström, R. Zorro, J. Blomgren, A. Hakansson, A. Ringbom, G. Tibell, O. Jonsson, L. Nilsson, P.U. Renberg, S.Y. van der Werf, W. Unkelbach, and F.P. Brady, Nucl. Phys. A 563 (1993) 225.

[5] S. El-Kateb, K.P. Jackson, W.P. Alford, R. Abbeg, R.E. Azuma, B.A. Brown, A. Celler, D. Frekers, O. Häusser, R. Helmer, R.S. Henderson, K.H. Hicks, R. Jeppesen, J.D. King, K. Raywood, G.G. Shute, B.M. Spicer, A. Trudel, M. Vetterli, and S. Yen, Phys. Rev. C 49 (1994) 3128.

[6] A.L. Williams, W.P. Alford, E. Brash, B.A. Brown, S. Burzynski, H.T. Fortune, O. Häusser, R. Helmer, R. Henderson, P.P. Hui, K.P. Jackson, B. Larson, M.G. McKinzie, D.A. Smith, A. Trudel, and M. Vetterli, Phys. Rev. C 51 (1995) 1144.

[7] W.P. Alford, B.A. Brown, S. Burzynski, A. Celler, D. Frekers, R. Helmer, R. Henderson, K.P. Jackson, K. Lee, A. Rahav, A. Trudel, and M. Vetterli, Phys. Rev. C 48 (1993) 2818.

[8] P.B. Radha, D.J. Dean, S.E. Koonin, K. Langanke, and P. Vogel, Phys. Rev. C 56 (1997) 3079; D.J. Dean, K. Langanke, L. Chatterjee, P.B. Radha, M.R. Strayer, Phys. Rev. C 58 (1998) 536.

[9] E. Caurier, G. Martínez-Pinedo, A. Poves, and A.P. Zuker, Phys. Rev. C 52 (1995) R1736; K. Langanke and G. Martínez Pinedo, Nucl. Phys. A 673 (2000) 481.

[10] E. Caurier, K. Langanke, G. Martínez-Pinedo, and F. Nowacki, Nucl. Phys. A 653 (1999) 439.

[11] J.A. Halbleib and R.A. Sorensen, Nucl. Phys. A 98 (1967) 542.

[12] J. Krumlinde and P. Möller, Nucl. Phys. A 417 (1984) 419; P. Möller and J. Randrup, Nucl. Phys. A 514 (1990) 1.

[13] G.F. Bertsch and S.F. Tsai, Phys. Rep. 18 (1975) 127; J. Suhonen, T. Taigel, and A. Faessler, Nucl. Phys. A 486 (1988) 91; N. Van Giai, Ch. Stoyanov, and V.V. Voronov, Phys. Rev. C 57 (1998) 1204; J. Engel, M. Bender, J. Dobaczewski, W. Nazarewicz, and R. Surnam, Phys. Rev. C 60 (1999) 014302.

[14] P. Sarriuguren, E. Moya de Guerra, A. Escuderos, and A.C. Carrizo, Nucl. Phys. A 635 (1998) 55.

[15] J. Engel, P. Vogel, and M.R. Zirnbauer, Phys. Rev. C 37 (1988) 731; V.A. Kuz'min and V.G. Soloviev, Nucl. Phys. A 486 (1988) 118; K. Muto and H.V. Klapdor, Phys. Lett. B 201 (1988) 420.

[16] K. Muto, E. Bender, and H.V. Klapdor, Z. Phys. A 333 (1989) 125; M. Hirsch, A. Staudt, K. Muto, and H.V. Klapdor-Kleingrothaus, Nucl. Phys. A 535 (1991) 62; K. Muto, E. Bender, T. Oda, and H.V. Klapdor-Kleingrothaus, Z. Phys. A 341 (1992) 407.

[17] H. Homma, E. Bender, M. Hirsch, K. Muto, H.V. Klapdor-Kleingrothaus, and T. Oda, Phys. Rev. C 54 (1996) 2972.

[18] P. Möller, J.R. Nix, and K.L. Kratz, At. Data Nucl. Data Tables 66 (1997) 131; J.U. Nabi and H.V. Klapdor-Kleingrothaus, At. Data Nucl. Data Tables 71 (1999) 149.

[19] P. Sarriuguren, E. Moya de Guerra, and A. Escuderos, Nucl. Phys. A 658 (1999) 13.

[20] P. Sarriuguren, E. Moya de Guerra, and A. Escuderos, Nucl. Phys. A 691 (2001) 631.

[21] P. Sarriuguren, E. Moya de Guerra, and A. Escuderos, Phys. Rev. C 64 (2001) 064306.

[22] M. Vallières and D.W.L. Sprung, Can. J. Phys. 56 (1978) 1190.

[23] D. Vautherin and D. M. Brink, Phys. Rev. C 5 (1972) 626; D. Vautherin, Phys. Rev. C 7 (1973) 296.

[24] G. Audi and A.H. Wapstra, Nucl. Phys. A 595 (1995) 409; G. Audi, O. Bersillon, J. Blachot, and A.H. Wapstra, Nucl. Phys. A 624 (1997) 1.

[25] H. Flocard, P. Quentin, A.K. Kerman, and D. Vautherin, Nucl. Phys. A 203 (1973) 433.

[26] N. Van Giai and H. Sagawa, Phys. Lett. B 106 (1981) 379.

[27] M. Beiner, H. Flocard, N. Van Giai, and P. Quentin, Nucl. Phys. A 238 (1975) 29.

[28] A. Chabanat, P. Bonche, P. Haensel, J. Meyer, and R. Schaeffer, Nucl. Phys. A 635 (1998) 231.

[29] H. de Vries, C.W. de Jager and C. de Vries, At. Data Nucl. Data Tables 36 (1987) 495.

[30] P. Raghavan, At. Data Nucl. Data Tables 42 (1989) 189; N.J. Stone, Oxford University, preprint (2001).

[31] N. Auerbach, G.F. Bertsch, B.A. Brown, and L. Zhao, Nucl. Phys. A 556 (1990) 190.

[32] P. Sarriuguren, E. Moya de Guerra, and R. Nojarov, Phys. Rev. C 54 (1996) 690; P. Sarriuguren, E. Moya de Guerra, and R. Nojarov, Z. Phys. A 357 (1997) 143.

[33] A. Bohr and B. Mottelson, *Nuclear Structure*, (Benjamin, New York, 1975).

[34] B. Castel and I.S. Towner, *Modern Theories of Nuclear Moments*, (Clarendon Press, Oxford, 1990).

[35] M. Hirsch, A. Staudt, K. Muto, and V. Klapdor-Kleingrothaus, At. Data Nucl. Data Tables 53 (1993) 165

[36] J. Rapaport, T. Taddeucci, T.P. Welch, C. Gaarde, J. Larsen, D.J. Horen, E. Sugarbaker, P. Koncz, C.C. Foster, C.D. Goodman, C.A. Goulding, and T. Masterson, Nucl. Phys. A 410 (1983) 371.

[37] B.D. Anderson, C. Lebo, A.R. Baldwin, T. Chitrakarn, R. Madey, J.W. Watson, and C.C. Foster, Phys. Rev. C 41 (1990) 1474.

Table 1. Comparison of the experimental charge radii [fm] [29] and quadrupole moments [b] [30] with the calculated values obtained with the force SG2.

	r_c exp	r_c calc	Q_0 exp	Q_0 calc
^{54}Fe	$3.675 - 3.732$	3.72	$+0.18(49)$	+0.46
^{56}Fe	$3.721 - 3.801$	3.74	$+0.81(10)$	+0.74
^{58}Ni	$3.769 - 3.772$	3.81	$+0.35(21)$	+0.40
^{60}Ni	$3.793 - 3.797$	3.84	$-0.11(17)$	-0.64
^{62}Ni	$3.822 - 3.830$	3.87	$-0.18(42)$	-0.80
^{64}Ni	$3.845 - 3.907$	3.88	$-1.4(7)$	-0.60

Table 2. Comparison of the GT_+ strengths in the energy range experimentally available (E_{ex}) between experimental [3–7] measurements and theoretical calculations.

	exp	HF+BCS	HF+BCS+pnQRPA
^{51}V	$1.2 \pm 0.1 (E_{ex} \leq 8 \text{ MeV})$	2.03	1.61
^{54}Fe	$3.5 \pm 0.7 (E_{ex} \leq 9 \text{ MeV})$	5.14	4.24
^{55}Mn	$1.7 \pm 0.2 (E_{ex} \leq 8.5 \text{ MeV})$	2.72	2.18
^{56}Fe	$2.9 \pm 0.3 (E_{ex} \leq 8.5 \text{ MeV})$	4.16	3.24
^{58}Ni	$3.8 \pm 0.4 (E_{ex} \leq 8.5 \text{ MeV})$	6.19	5.00
^{59}Co	$1.9 \pm 0.1 (E_{ex} \leq 8 \text{ MeV})$	3.26	2.50
^{60}Ni	$3.11 \pm 0.08 (E_{ex} \leq 8 \text{ MeV})$	4.97	3.72
^{62}Ni	$2.53 \pm 0.07 (E_{ex} \leq 8 \text{ MeV})$	3.40	2.36
^{64}Ni	$1.72 \pm 0.09 (E_{ex} \leq 8 \text{ MeV})$	2.65	1.65

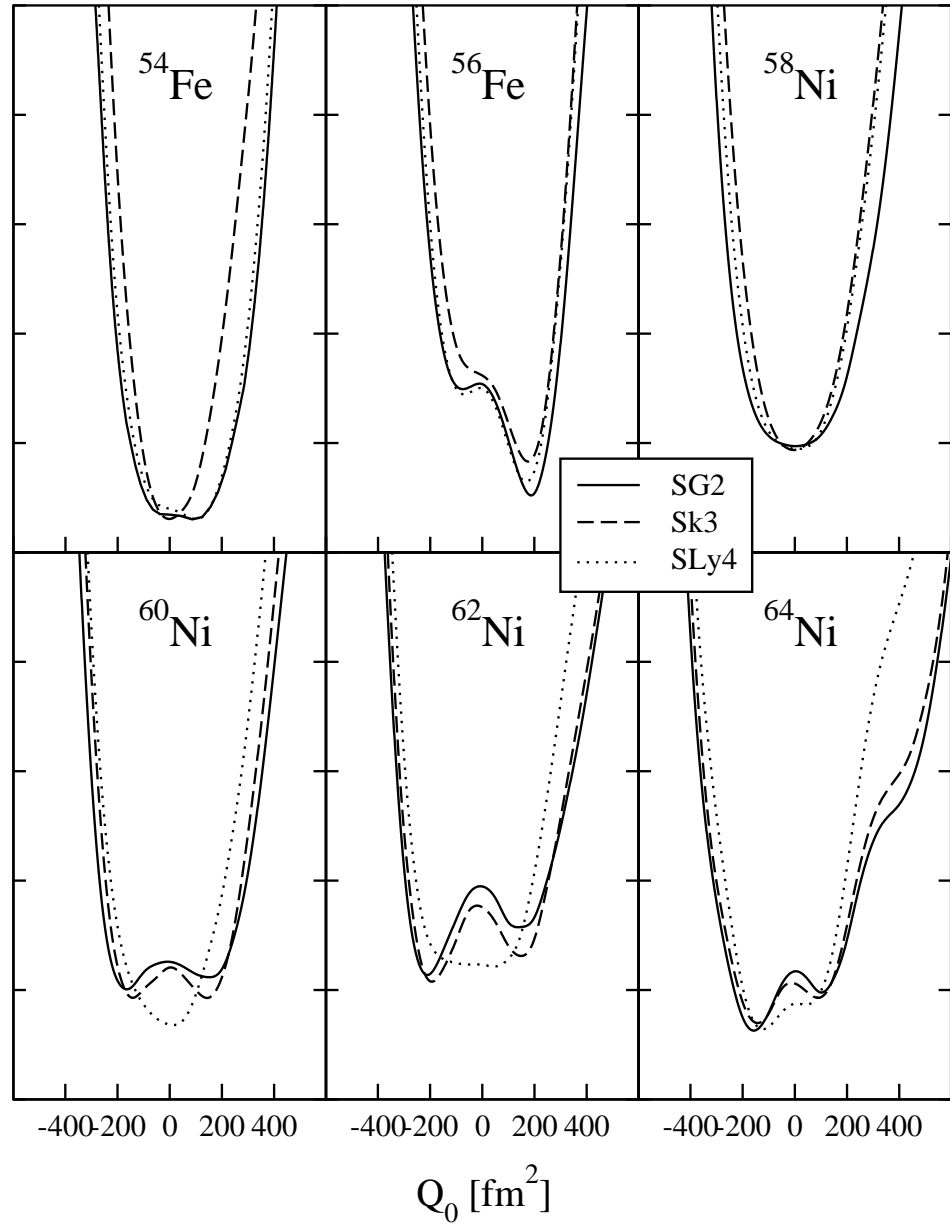


FIG. 1. Total energy as a function of the mass quadrupole moment Q_0 obtained from a constraint HF+BCS calculation with three Skyrme forces SG2, Sk3, and SLy4.

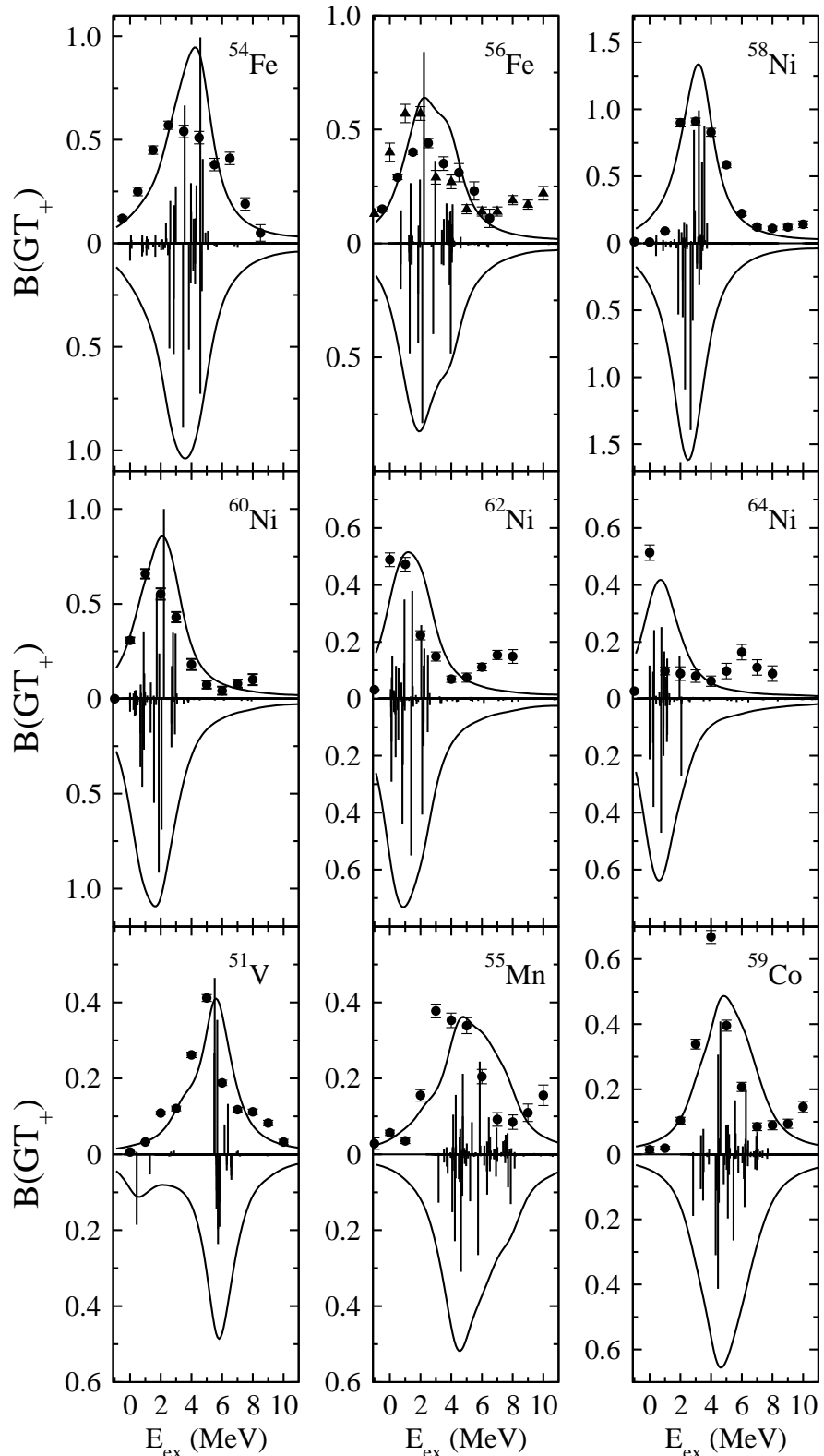


FIG. 2. Gamow-Teller strength distributions (GT_+) plotted versus the excitation energy of the corresponding daughter nucleus. The results are plotted downward in the case of HF+BCS approximation and upward in the case of HF+BCS+pnQRPA. Experimental data are from Refs. [3-7].

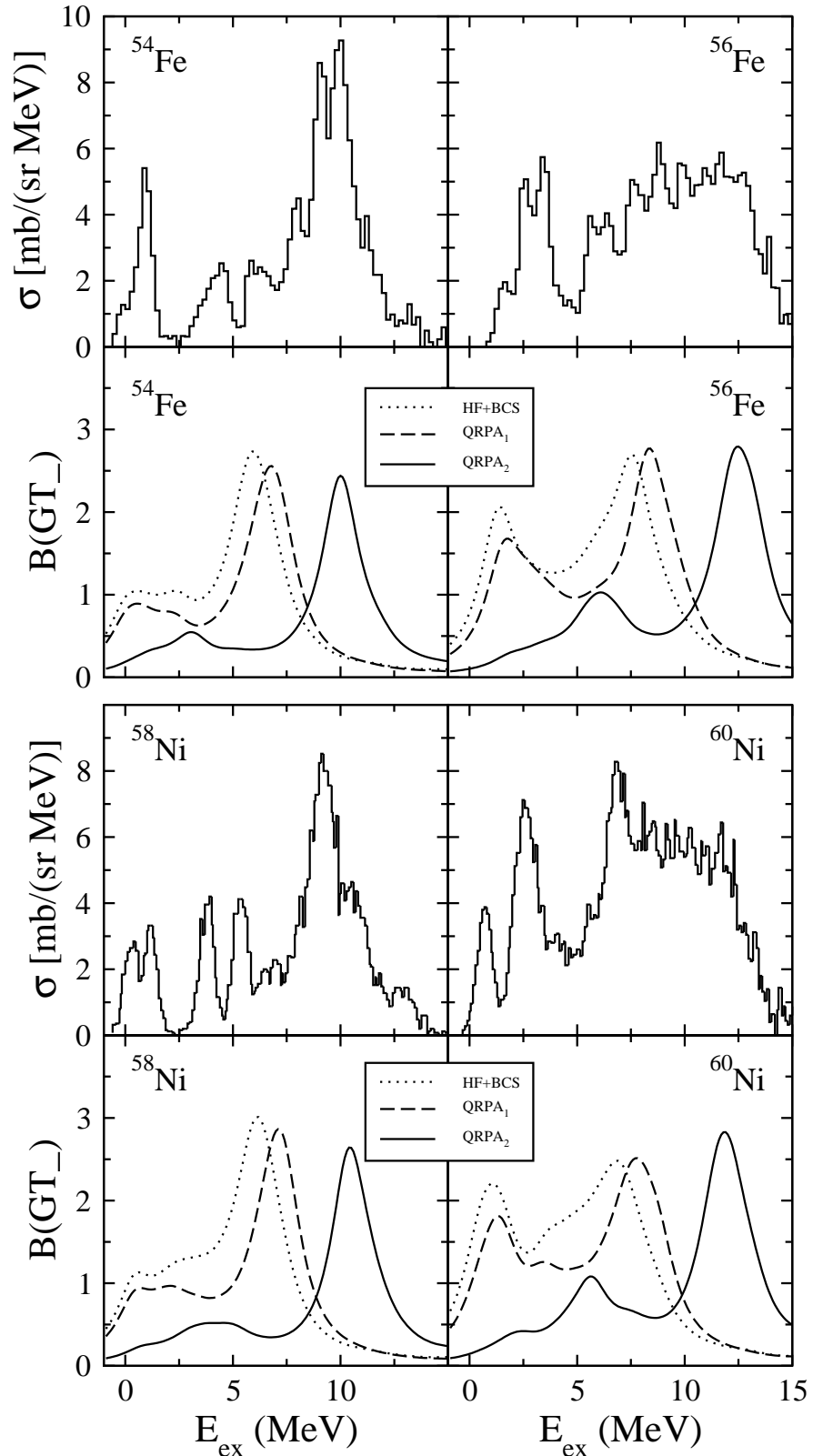


FIG. 3. Comparison of (p,n) $L = 0$ forward-angle cross section data [37] (upper panels) with the calculated Gamow-Teller strength distributions (GT_-) as a function of the excitation energy of the daughter nucleus [MeV].